

# The stellar populations of the Fornax dwarf spheroidal galaxy. <sup>\*</sup>

Ivo Saviane<sup>1</sup>, Enrico V. Held<sup>2</sup>, and Gianpaolo Bertelli<sup>3,1</sup>

<sup>1</sup> Università di Padova, Dipartimento di Astronomia, vicolo dell'Osservatorio 5, I-35122 Padova, Italy

<sup>2</sup> Osservatorio Astronomico di Padova, vicolo dell'Osservatorio 5, I-35122 Padova, Italy

<sup>3</sup> Consiglio Nazionale delle Ricerche, CNR-GNA, Roma, Italy

**Abstract.** We present  $B, V, I$  CCD photometry of about 40000 stars in four regions of the Fornax dwarf spheroidal galaxy down to  $V \sim 23.5$ , the largest three-color data set obtained for this galaxy until now. The resultant color-magnitude diagrams, based on a wide color baseline, show a variety of features tracing the history of star formation of this dwarf galaxy. One of the most distinctive features in our diagrams is the conspicuous young main sequence, indicating recent star formation until approximately  $2 \times 10^8$  yr ago. A plume of stars brighter than the red HB clump, with  $(B - I) \sim 0.5$ , trace the helium-burning phase of the young population. A comparison of the color and extension of this feature with model isochrones suggests a relatively metal-rich population ( $[\text{Fe}/\text{H}] \sim -0.7$ ) with age 300–400 Myr. This represents an important constraint for understanding the chemical enrichment history of Fornax. An extended upper AGB tail and a prominent red HB clump sign the presence of the well-known dominant intermediate-age population with an age range 2–10 Gyr, for which we have estimated a mean age  $5.4 \pm 1.7$ . About 0.2 mag below the red clump, an extended HB is indicative of an old population. We show that blue HB stars may be present in the outer regions. Together with previous detection of RR Lyrae, this provides evidence for a minority field population that is as old and metal-poor as that in the Fornax globular clusters. We have identified the AGB bump, a clustering of stars that occurs at the beginning of helium shell-burning evolution, at a luminosity  $M_V \simeq -0.4$ . This is an example of the short-lived evolutionary phases that can be revealed in stellar populations using adequately large star data samples, whose measurements provide powerful tests of theoretical models.

Based on precise detection of the tip of the RGB in a selected RGB sample, we measure a corrected distance modulus  $(m - M)_0 = 20.70 \pm 0.12$ . An independent estimate of the distance to Fornax was also obtained from the mean magnitude of old horizontal branch stars, yielding a distance modulus  $(m - M)_0 = 20.76 \pm 0.04$ , in good agreement with the distance estimated from the red giant branch tip and previous results. The large baseline of the  $(B - I)$  colors together with the size

of the stellar sample allowed us to analyze in detail the color distribution of the red giant stars. We find that it can be approximately described as the superposition of two populations. The dominant component, comprising  $\sim 70\%$  of the red giant stars, consists of relatively metal-enriched intermediate-age stars. Its mean metallicity is  $[\text{Fe}/\text{H}] = -1.39 \pm 0.15$ , based on a comparison of the fiducial locus of the bulk of the Fornax red giants with the homogeneous Galactic globular cluster set of Da Costa & Armandroff (1990). Once the younger mean age of Fornax is taken into account, our best estimate for the mean abundance of the bulk of the galaxy is  $[\text{Fe}/\text{H}] \approx -1.0 \pm 0.15$ . The dominant intermediate-age component has an intrinsic color dispersion  $\sigma_0(B - I) = 0.06 \pm 0.01$  mag, corresponding to a relatively low abundance dispersion,  $\sigma_{[\text{Fe}/\text{H}]} = 0.12 \pm 0.02$  dex. Further, there is a distinct small population of red giants on the blue side of the RGB. While these stars could be either old or young red giants, we show that their spatial distribution is consistent with the radial gradient of old horizontal branch stars, and completely different from that of the younger population. This unambiguously qualifies them as old and metal-poor. This result clarifies the nature of the red giant branch of Fornax, suggesting that its exceptional color width is due to the presence of two main populations yielding a large abundance range ( $-2.0 < [\text{Fe}/\text{H}] < -0.7$ ). This evidence suggests a scenario in which the Fornax dSph started forming a stellar halo and its surrounding clusters together about 10–13 Gyr ago, followed by a major star formation epoch (probably with a discontinuous rate) after several Gyr.

**Key words:** Galaxies: fundamental parameters – Galaxies: individual: Fornax – Local Group – Galaxies: stellar content – Galaxies: structure

## 1. Introduction

An increasingly large number of investigations has recognized the importance of dwarf spheroidal galaxies for our understanding of galaxy formation and evolution (see Mateo 1998 and Da Costa 1998 for recent reviews). While new studies of the central, densest regions of the more distant Local Group galaxies have benefited from the exceptional resolution of HST,

Send offprint requests to: E. V. Held (held@pd.astro.it)

<sup>\*</sup> Based on data collected at the European Southern Observatory, La Silla, Chile, Proposal N. 56.A-0538

the nearby dwarf spheroidal satellites of the Milky Way can still be investigated in great detail using ground based wide-field data. Thanks to recent improvements in detector efficiency (in particular, in the blue part of the optical spectrum) and size, CMD's with long color baselines and high statistical significance can be obtained in affordable exposure times.

The Fornax dwarf spheroidal (dSph) galaxy represents one of the most interesting cases for studying the complexity of stellar populations in dwarf galaxies. This galaxy was one of the first dSph in which an intermediate age population was detected. The presence of upper asymptotic giant branch (AGB) stars, brighter and redder than the tip of the red giant branch (RGB), indicated that about 20% of the galaxy could be of intermediate age (2 to 8 Gyr) (Aaronson & Mould 1980, 1985). Surveys for AGB stars led to discovery of 111 carbon stars, for which follow up near-infrared photometry indicated a wide range of bolometric luminosities, a mass dispersion among the progenitors, and hence an age spread (Frogel et al. 1982; Westerglund et al. 1987; Lundgren 1990; Azzopardi et al. 1999). Fornax is also known to contain a planetary nebula whose abundance patterns are consistent with an origin from a second or third generation star (Danziger et al. 1978; Maran et al. 1984). The presence of such an intermediate-age population is confirmed by a conspicuous red HB clump (Demers et al. 1994; Stetson et al. 1998). Most recently, an HST study of a central Fornax field sampling the main-sequence turnoffs of the intermediate-age and old populations has been carried out by Buonanno et al. (1999). The analysis of the resulting CMD has shown evidence for a star formation starting about 12 Gyr ago and continuing until 0.5 Gyr ago. A variable star formation rate is revealed by gaps between separate subgiant branches, and major star formation episodes probably occurred nearly 2.5, 4, and 7 Gyr ago.

Also, Fornax certainly harbors an old stellar population, since it contains five globular clusters whose ages do not differ from those of M68 and M92 (Buonanno et al. 1998; Smith et al. 1998), except perhaps for cluster 4 that appears to be 2-3 Gyr younger (Buonanno et al. 1999). These clusters have unusually red horizontal branches for their low metallicity, with no counterparts in the outer Galactic halo or the Magellanic Clouds. Also for cluster 4, the recent WFPC2 color-magnitude diagrams of Buonanno et al. (1999) unambiguously indicate a low metallicity,  $[Fe/H] \approx -2$ , although integrated spectra pointed to a metallicity similar to that of field stars (Beauchamp et al. 1995). An old population is present among the field stars of Fornax as well, as demonstrated by detection of a red horizontal branch slightly fainter than the red clump, and of RR Lyrae variables (Buonanno et al. 1985; Stetson et al. 1998, hereafter SHS98).

Fornax also hosts a significant population of young stars. Buonanno et al. (1985) had already noticed a handful of faint blue stars in their CMD of the Fornax field, tentatively explained as belonging to a  $\sim 2 \times 10^9$  yr population (cf. also Gratton et al. 1986). The deeper CMD of Beauchamp et al. (1995) clearly revealed a young main-sequence, and comparison with theoretical isochrones indicated recent star formation. The brightest

turnoff was located at  $M_V \simeq -1.4$ , implying a minimum age of  $\sim 10^8$  yr. This young population is best shown by the recent wide-area survey of SHS98. Notwithstanding this young stellar component, Fornax appears to be devoid of any interstellar medium (ISM). A large-area search for neutral hydrogen has given no detectable HI emission or absorption (Young 1999), the upper limit for HI emission being  $5 \times 10^{18} \text{ cm}^{-2}$  at the galaxy center. Thus the interstellar medium that must have been present a few  $10^8$  yr ago to form stars, appears to be all gone. There is also the possibility that the ISM has been ionized and heated up by the interstellar UV field. However, this hypothesis conflicts with the lack of detection of X-ray emission in the direction of Fornax (Gizis et al. 1993).

The various stellar subpopulations in Fornax have different spatial distributions, which have been carefully investigated by SHS98. The oldest population, represented by the RR Lyrae variables, has the most extended distribution. The intermediate-age stars (red clump stars) are more centrally concentrated, while the young population of blue MS stars, as well the reddest AGB (carbon) stars, are even more concentrated in a bar-like distribution roughly aligned in the EW direction, with the brightest stars located at the ends of the bar. Also the red clump population displays an asymmetrical structure (cf. Hodge 1961; Eskridge 1988; Demers et al. 1994), with a peculiar ‘‘crescent’’ shape (SHS98).

Despite all these pieces of knowledge accumulated in recent years, the star formation history of Fornax is not yet fully understood. Several questions need to be answered before a reconstruction of the star formation and chemical enrichment history of Fornax can be attempted. The metallicity should be measured for stellar populations of different age and location within the galaxy, so as to determine the run of metal enrichment as a function of time. The star formation history needs to be evaluated using critical features in the CMD as tracers of star formation at different epochs, to understand to what extent star formation proceeded continuously or in bursts, and how it propagated throughout the body of the galaxy. The nature of the wide red giant branch (RGB) is still quite puzzling, though all previous investigations agree on the fact that it is broader than expected on the basis of the photometric errors. Further, there is a lack of observational data with which to study features such as the RGB and AGB bumps or the precise location of central helium-burning stars as a function of age and metal abundance, as a test of stellar evolution models. Large field observations of Local Group dSph galaxies, being able to sample a significant number of stars, can address these issues.

With these open questions in mind, we have investigated the stellar populations of Fornax as part of a wide-field study of nearby dwarf spheroidals. We present here a large area *BVI* photometric study of the Fornax field, yielding magnitudes and colors for about 40,000 stars down to  $\sim 2$  mag below the horizontal branch, in four regions located at different distances from the galaxy center. The use of standard passbands, together with the size of our stellar sample, allowed us to derive the basic physical properties of Fornax with high accuracy and mea-

**Table 1.** The journal of observations

Nt.	ID	Filter	$t_{\text{exp}}[\text{s}]$	$X$	FWHM["']
19 Oct. 1995	A	<i>B</i>	3×900	1.02	1.5
19 Oct. 1995	A	<i>I</i>	3×900	1.11	1.5
19 Oct. 1995	A	<i>V</i>	3×900	1.06	1.7
20 Oct. 1995	B	<i>B</i>	3×1200	1.09	1.5
20 Oct. 1995	B	<i>I</i>	1200	1.01	1.3
19 Oct. 1995	B	<i>V</i>	600	1.26	1.4
20 Oct. 1995	B	<i>V</i>	2×600	1.22	1.4
21 Oct. 1995	C	<i>B</i>	3×1200	1.25	1.5
21 Oct. 1995	C	<i>I</i>	3×1200	1.03	1.3
20 Oct. 1995	C	<i>I</i>	240	1.11	1.0
21 Oct. 1995	C	<i>V</i>	3×600	1.10	1.6
20 Oct. 1995	D	<i>B</i>	1200	1.34	1.5
21 Oct. 1995	D	<i>B</i>	2×1200	1.03	1.5
21 Oct. 1995	D	<i>I</i>	3×1200	1.01	1.3
21 Oct. 1995	D	<i>V</i>	3×600	1.11	1.6
21 Oct. 1995	BKG	<i>B</i>	1800	1.15	1.6
21 Oct. 1995	BKG	<i>I</i>	1500	1.24	1.4
21 Oct. 1995	BKG	<i>V</i>	900	1.36	1.8

sure details in its CMD that trace the less numerous populations and faster evolutionary phases.

In particular, the *B* band turned out to be invaluable for studying the hot stars, be they old or young, whereas the wide baseline of the  $(B - I)$  color provides the best resolution of the different evolutionary phases in the color-magnitude diagrams (cf. Smecker-Hane et al. 1994; Held et al. 1999). Also, the availability of a comparison field allowed us to estimate the foreground and background contamination. The present photometry will be the input database to model the star formation history (SFH) of Fornax (Held et al., in preparation) using population synthesis techniques.

The paper is organized as follows. The observations and data reduction are presented in Sect. 2. In Sect. 3 we present *V*,  $(B - I)$  color-magnitude diagrams of the Fornax field stars and discuss several interesting features with the help of theoretical isochrone fitting. The *V*, *I* luminosity function is derived in Sect. 4.1 and used to estimate the distance to Fornax. This is confirmed by an independent distance estimate based on the *V* luminosity of old-HB stars (Sect.4.2). In Sect. 4.3 we compare the CMD of Fornax with template globular cluster RGB sequences using the standard  $(V - I)$  colors, and discuss the mean abundance and age of the dominant population. The color distribution of red giant stars in Fornax is analyzed in detail in Sect. 4.4, where the size of an intrinsic abundance spread is discussed. Some light on the nature of the wide RGB of Fornax is shed by a comparison of the spatial gradient of different populations (Sect. 4.5). Our results and conclusions are summarized in Sect. 5.

## 2. Observations and data reduction

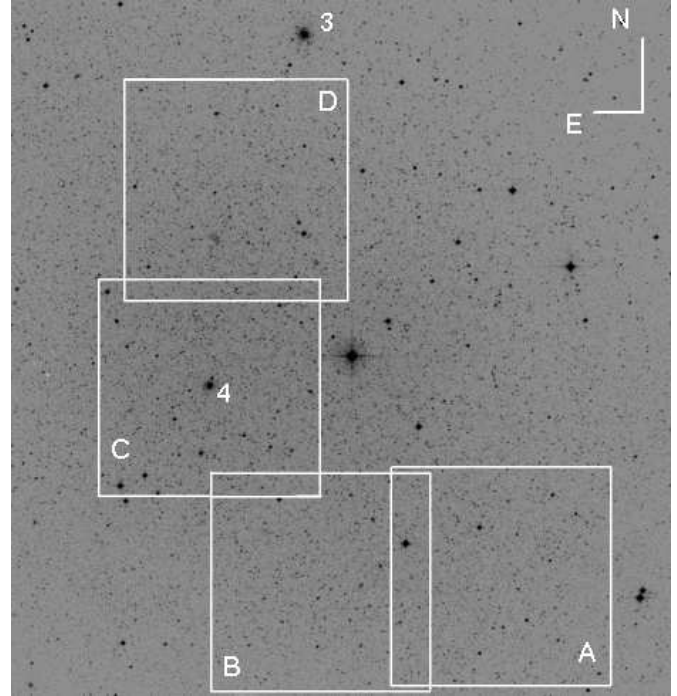


**Fig. 1.** The central area of Fornax reproduced from the Palomar Digital Sky Survey. The squares indicate the  $10'.7 \times 10'.7$  regions studied in this paper. The Fornax globular clusters #3 and #4 are also indicated

### 2.1. Observations

The Fornax galaxy was observed on October 19–21, 1995 using DFOSC at the ESO/Danish 1.54m telescope. The detector was a  $2048 \times 2048$  Loral CCD with pixel  $0''.40$ , covering a field of view of  $13'.6 \times 13'.6$ . Due to non-uniform sensitivity near the edges of the CCD, the images were trimmed to a useable area of  $1600 \times 1600$  pixels (i.e.  $10'.7 \times 10'.7$ ). CCD readout by amplifier B in high-gain mode yielded a noise of  $7.2 e^-/\text{px}$  (rms) and a conversion factor of  $1.31 e^-/\text{ADU}$ .

We observed 4 slightly overlapping fields in Fornax, plus one control field. A map of the location of the fields is shown in Fig. 1. The innermost field (region C) is centered on the globular cluster #4, i.e. at about 4 arcmin from the galaxy center (as defined by SHS98). The outermost field (A) is located at  $\sim 13'.5$  from the center. The journal of the observations is reported in Table 1. The columns give the night, an image identifier, the filter, exposure time and airmass, and the FWHM of the point spread function (PSF). The seeing was only fair, yet adequate to measure the relatively bright stars in our database. The third night had the most stable weather conditions. Several short exposure images, not included in this table, were used for checking the photometric zero points.

### 2.2. Reduction and photometry

The image processing was carried out with the ESO/MIDAS package in a standard way. Reduction follows the procedures detailed by Saviane et al. (1996, Paper I) and Held et al. (1999,

Paper II). For each field/filter combination, master images were produced by registering and coadding the long exposure images. The PSF was not significantly degraded by this process. Stellar photometry was performed using DAOPHOT and ALLSTAR (Stetson 1987). The final PSF star catalogs contained  $\simeq 50$  stars, and the best fit was obtained by fitting a Moffat ( $\beta = 1.5$ ) function with a quadratic dependence on the  $x$ ,  $y$  star coordinates. ALLSTAR was run twice on the sum images. In the second run, the star subtracted frames were searched for faint undetected objects that were added to the input lists of stars. The master photometric catalogs were created using the complete lists of stars as new inputs to ALLSTAR.

### 2.3. Calibration

Observations of Landolt's (1992) standard star fields were used to calibrate the photometry. The raw magnitudes were first normalized according to the following equation

$$m' = m_{\text{ap}} + 2.5 \log(t_{\text{exp}} + \Delta t) - k_{\lambda} X \quad (1)$$

where  $m_{\text{ap}}$  are the instrumental magnitudes measured in a circular aperture of radius  $R = 6''.9$ ,  $\Delta t$  is the shutter delay and  $X$  the airmass. A shutter delay of  $-0.11$  s was estimated from a sequence of images taken with increasing exposure times. The extinction coefficients  $k_B = 0.235$ ,  $k_V = 0.135$  and  $k_I = 0.048$  were adopted from the Geneva Observatory Photometric Group data. The normalized instrumental magnitudes were then compared to Landolt's (1992) values, and the following relations were found:

$$B = b' + 0.207(B - V) + a_B \quad (2)$$

$$V = v' + 0.0544(B - V) + a_V \quad (3)$$

$$V = v' + 0.0489(V - I) + c_V \quad (4)$$

$$I = i' - 0.00658(V - I) + a_I \quad (5)$$

where  $a_B = 23.041$ ,  $23.025$  and  $23.038$  for the nights 1, 2 and 3, respectively. In the same order of nights, the other coefficients are  $a_V = 23.774$ ,  $23.763$  and  $23.772$ ;  $c_V = 23.772$ ,  $23.762$  and  $23.771$ ; and finally  $a_I = 23.070$ ,  $23.054$  and  $23.077$ . The standard deviations of the residuals were  $0.018$ ,  $0.013$ , and  $0.022$  mag in  $B$ ,  $V$  (both equations), and  $I$  respectively.

The PSF magnitudes were scaled to aperture magnitudes by assuming that  $m_{\text{ap}} = m_{\text{PSF}} + \text{const.}$  (Stetson 1987). Aperture magnitudes were measured for a sample of bright, isolated stars, and for each star we computed the difference with respect to the PSF magnitude measured on the coadded frames. The same reference aperture used for the standard stars was employed. The internal calibration uncertainty due to ‘‘aperture correction’’, estimated from the consistency of the zero point derived from several individual images, is of the order  $0.01$  mag for all filters.

The instrumental magnitudes and colors for the stars observed in at least two filters were calibrated either with an it-

erative procedure or by solving a system of 3 equations of the form

$$m_{\text{std}} = m_{\text{inst}} + k_m \text{color}_{\text{std}} + a_m$$

where  $m_{\text{std}}$  and  $\text{color}_{\text{std}}$  are the magnitude and color in the standard system, and  $m_{\text{inst}}$  are the instrumental magnitudes.

After independent calibration, we performed a verification of the photometric zero points of the catalogs in the 4 zones by comparing stars in the overlap strips. Since the mean systematic deviations between  $BVI$  magnitudes measured in the field C and D (both observed during the third, most stable night) are less than  $0.03$  mag, we chose to refer all photometry to the zero point of the central field C, and applied small zero-point corrections to our photometry in the field A, B, and D. We conservatively adopt an uncertainty of  $0.03$  mag as our systematic error in all bands.

### 2.4. Comparison with previous studies

As a further check of the accuracy of our photometric zero point, we compared our results with previous data in the literature. The only published photometry tables are those of Buonanno et al. (1985). Their Tables 6 and 7 report the values of  $V$  and  $(B - V)$  for all the stars measured in two separate  $2 \times 2$  arcmin<sup>2</sup> fields, called A1 and A2, which are included in our fields C and A. The two sets of measurements for the A2-A field pair are in good agreement. The median differences (this paper – Buonanno et al.) are  $-0.013$  in  $V$  and  $-0.017$  in  $B - V$ , with standard deviations of  $0.16$  mag in both cases.

The consistency between the zero-points for the A1-C pair is still good, yielding median residuals  $0.014$  ( $\sigma = 0.20$ ) in  $V$  and  $0.024$  ( $0.25$ ) in  $B - V$ .

### 2.5. Artificial star tests

Extensive artificial star simulations were performed to evaluate the uncertainties of our photometry and the completeness of the data. The simulations were carried out for the fields A and C, which represent the lowest and highest crowding in our frames. A list of input stars was created for each  $V$  master image, with uniformly distributed magnitudes. The star coordinates were generated over a grid of triangles with a small random offset from the vertices, a configuration allowing to add the largest number of non-overlapping simulated stars. Error estimates based on randomly placed artificial stars may not be realistic if there is a significant amount of clustering among real stars. This caveat does not seem to apply to our relatively uniform Fornax fields, though.

The same artificial stars were used in all bands, using random  $(B - V)$  and  $(V - I)$  colors so that the stars were uniformly distributed in the color-magnitude diagrams. We typically added  $\sim 36000$  stars per filter in 80 experiments. The frames with the artificial stars were then reduced using exactly the same procedures as for the original images. For each filter, the retrieved artificial stars were matched to the input list

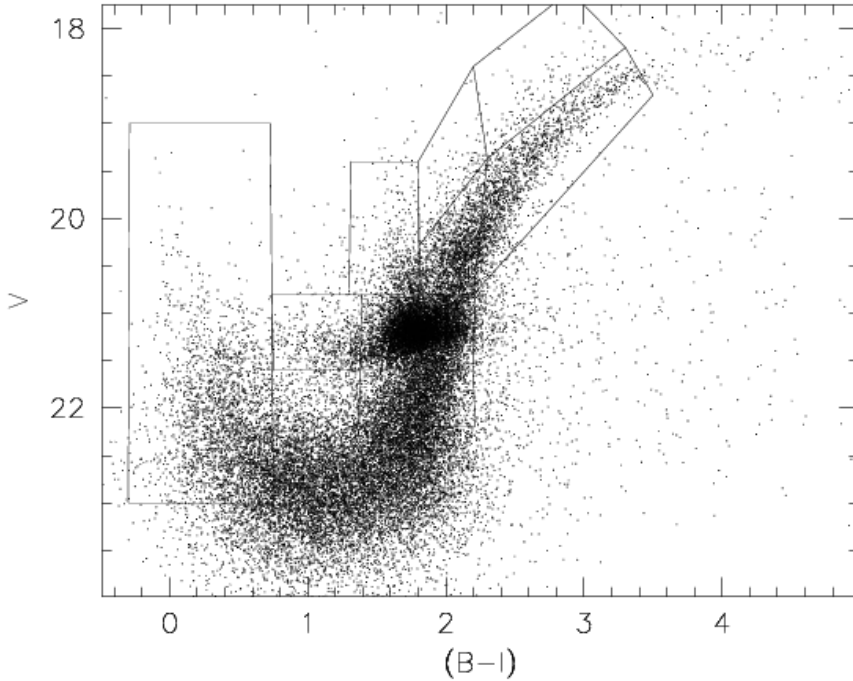


**Fig. 2.** The color-magnitude diagram of Fornax in the  $(B - I), V$  plane. This diagram includes about 42500 stars in all fields. The most noticeable features are the wide RGB made of old and intermediate-age stars, the upper AGB tail, a young main sequence, and a prominent red clump together with fainter, older HB stars. The blue main sequence clearly merges into a mix of subgiant branches. The outlined regions have been used for counting stars in different evolutionary phases (*see text*)

**Table 2.** The photometric errors from artificial star experiments

$V, B, I$	$\sigma_V$	$\sigma_B$	$\sigma_I$	$\sigma_V$	$\sigma_B$	$\sigma_I$
	A			C		
14.75	...	...	0.003	...	...	...
15.25	...	...	0.003	...	...	...
15.75	...	...	0.003	...	...	0.011
16.25	...	...	0.004	...	...	0.012
16.75	...	...	0.005	...	...	0.014
17.25	...	0.013	0.006	...	0.010	0.017
17.75	...	0.014	0.013	0.014	0.014	0.018
18.25	0.013	0.014	0.017	0.016	0.019	0.019
18.75	0.017	0.019	0.020	0.020	0.018	0.026
19.25	0.021	0.024	0.028	0.025	0.023	0.032
19.75	0.024	0.031	0.037	0.032	0.030	0.045
20.25	0.030	0.038	0.049	0.040	0.036	0.064
20.75	0.038	0.052	0.069	0.061	0.049	0.082
21.25	0.057	0.069	0.098	0.081	0.064	0.108
21.75	0.073	0.085	0.144	0.103	0.082	0.156
22.25	0.107	0.105	0.150	0.136	0.106	...
22.75	0.116	0.134	0.181	...	0.124	...

by means of their coordinates. The stars recovered in different colors were matched, and the raw catalog calibrated just as the original photometry. The standard deviations of the measurement errors  $\Delta m$ , calculated in 0.5 mag bins, are given in Table 2. The first column gives the bin centers, columns 2 to 4 and 5 to 7 list the errors obtained for the fields A and C, respectively. The measured standard errors span a range from

$\simeq 0.01$  mag near the tip of the RGB to  $\simeq 0.15$  mag close to the limiting magnitudes. Errors and the limiting magnitudes are consistent with the different crowding conditions and exposure times in the two fields. Contour plots of the completeness levels were produced by dividing each CMD in cells with color and magnitude steps of 0.5 and 0.2 mag, respectively, and counting the artificial stars within each cell before and after reduction. We used the same acceptance criteria as for the galaxy's CMD, i.e. a star was counted in a cell only if it was recovered in each of the 3 filters. The completeness array was computed as the ratio between the post-reduction and the input simulated star counts, and median filtered with a  $5 \times 5$  box to reduce the noise in the contour plots. Examples of the resultant completeness contours will be shown in Sect. 3.

### 3. Color-magnitude diagrams

The combination of a wide photometric baseline and large sample size employed in this study allowed us a very detailed view of the evolved stellar populations in Fornax. Fig. 2 presents the  $V, (B - I)$  color-magnitude diagram of this nearby dwarf spheroidal, showing an excellent separation of stars in different evolutionary phases. We now briefly describe the many interesting features seen in this CMD.

- A wide red giants branch, comprising stars older than  $\sim 1$  Gyr. The color spread is much larger than expected from photometric errors (cf. Sect. 4.4). While the red side of the RGB shows a sharp edge, the stars are spread on the blue side forming sparsely populated sequences distinct from the RGB (cf. SHS98). This is more evident in Fig. 3. Note that the foreground and background contamination is virtually negligible in the relevant regions of the diagram. The

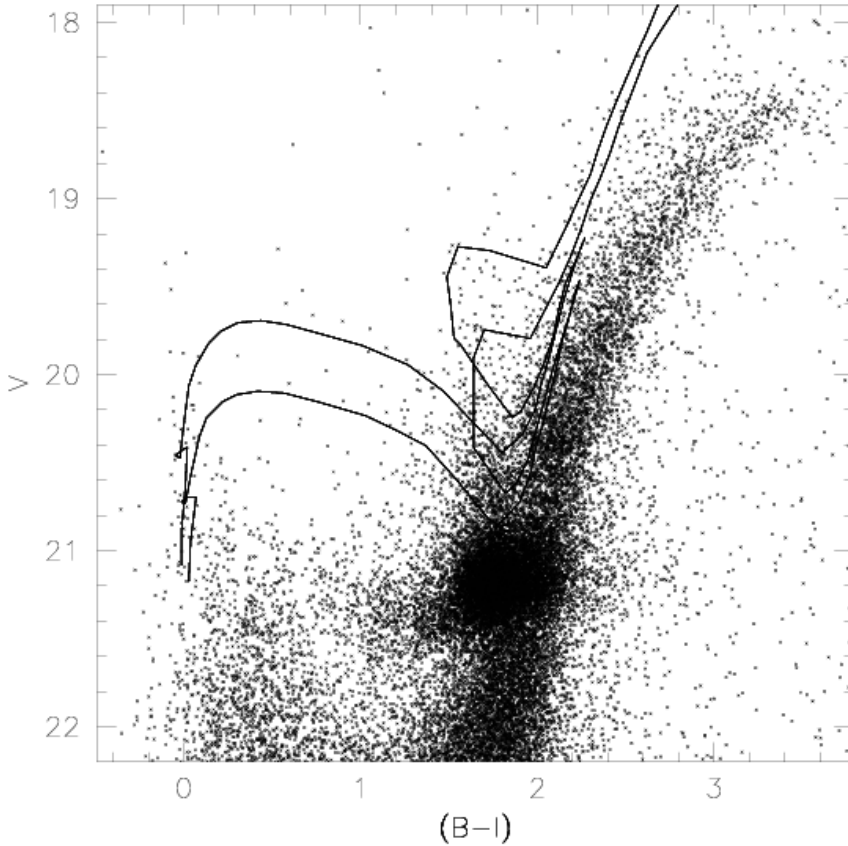


**Fig. 3.** An enlarged view of the color-magnitude diagram of Fornax showing the features produced by core helium-burning stars, and morphological details of the red giant branch. Two isochrones from the post-MS models of Bertelli et al. (1994) with  $Z=0.004$  and ages 300 and 400 Myr (top to bottom) have been superimposed to the data. The plume of stars above the red clump is composed of intermediate mass stars burning helium in the core after leaving the young main sequence.

color-magnitude diagram of foreground and background objects in our control field, covering an area  $10'.7 \times 10'.7$ , contains only 154 objects down to  $V \approx 22.5$ .

- Above the RGB tip at  $V \sim 18.4$ , there is a well-developed upper AGB tail extending to colors as red as  $(B - V)$  and  $(V - I) \sim 3$ , or  $(B - I) \sim 6$ . The upper AGB consists of intermediate-age C and M stars, the latter comprising a small group of stars just above the RGB tip (see SHS98).
- A rich red clump contains the majority of HB stars of a numerous intermediate-age and metal-enriched population; in the following we will refer to it simply as red clump (RC) (cf. Demers et al. 1994; SHS98). About 0.2 mag fainter, a horizontal branch originating from an older population is clearly seen, indicated in the following as “old HB” (or HB<sub>OLD</sub>). We also notice the instability strip mostly populated by RR Lyrae variables, whose random phase colors and magnitudes define a band  $\lesssim 1$  mag thick. RR Lyrae variables are present in the Fornax field (Buonanno et al. 1985; SHS98; Mateo 1998). Blue HB stars are hardly seen in this diagram. If any exist, they are confused with the young main sequence stars.
- A blue plume reaching  $V \sim 20$ , identified with a young main sequence of  $\sim 0.1$  Gyr old stars (Beauchamp et al. 1995; SHS98).
- An almost vertical plume originating from  $(B - I) \sim 1.8$ ,  $V \sim 21$ , i.e. just above the red clump, extending up to

$V \sim 19.3$ . They are, as it will be shown below, core helium-burning stars with mass in the range  $\sim 2 M_{\odot}$ .

- At fainter magnitudes, the main sequence merges into a heavily populated region  $\sim 1$  mag below the HB, involving a mix of subgiant branches of different ages.
- We also note the small clump of stars at  $V \sim 20.4$  on the red giant branch, an example of the short-lived evolutionary phases that can be revealed in stellar populations using adequately large data samples. This feature is identified with the AGB bump, a clumping of stars due to a slowing down of the luminosity increase at the beginning of AGB evolution (e.g., Gallart 1998; Alves & Sarajedini 1999). We will return on this point in Sect. 4.1.

Overall, this diagram shows that Fornax went on forming stars from an early epoch ( $> 10$  Gyr ago) until about 100 Myr ago. A closer picture of the CMD is presented in Fig. 3, showing details of the core helium-burning stars, which are important diagnostics of stars formation histories in galaxies. The prominent red clump comprises stars with age 2–10 Gyr and mass approximately 0.9 to  $1.4 M_{\odot}$ . Its mean luminosity and color bears information on the mean age of Fornax. We will return on this point later. A comparison with theoretical isochrones of Bertelli et al. (1994) allows one to establish the nature of the stars producing the plume above the RC. These are intermediate-mass core helium-burning stars ( $2.4\text{--}2.9 M_{\odot}$ ),

counterparts of the young main sequence stars in the age range 0.3–0.5 Gyr, which started burning helium in a non-degenerate core.

This stage (also known as the “blue-loops”) represents an important indicator of the metallicity of the young population and therefore of the chemical enrichment history of galaxies (e.g., Aparicio et al. 1996; Cole et al 1999; and references therein). Fig. 3 shows that fitting the RC plume requires isochrones having  $[\text{Fe}/\text{H}] \sim -0.7$ , i.e. significantly more metal-rich than the bulk of the Fornax stellar population. This relatively high metallicity of the younger stars may probably explain why Fornax seemingly lacks a large population of anomalous Cepheids (AC), which are so numerous in the metal-poor dSph Leo I (see discussion of the instability strip in Caputo et al. 1999). Searches of AC’s in Fornax are underway (Bersier & Wood 1999).

The color-magnitude diagrams for the innermost and outermost region in this study, shown in Fig. 4, illustrate the remarkable variation of the stellar populations in Fornax with galactocentric radius. The inner field (C, bottom panel) shows all of the features noticed in the total CMD. The young main-sequence stars are less numerous in the outer field, even accounting for the lower stellar surface density, and there are very few blue stars brighter than  $V \sim 22$ . The young core-He-burning stars (the plume above the RC) follow the trend of the blue main sequence stars. In contrast, it is interesting to note a hint of a *blue horizontal branch* in the outer field. Together with the detection of RR Lyrae stars, our data provide evidence for a small *old, metal-poor field population* similar to that of the Fornax globular clusters. A population II halo seems to be common not only in dwarf spheroidals (see Mateo 1998) but also in dwarf irregulars (e.g., Minniti et al. 1999; Aparicio et al. 1997). A quantitative estimate of the population gradient in Fornax will be given in Sect. 4.5.

## 4. Analysis and discussion

### 4.1. Luminosity function and distance

The red giant luminosity function (LF) and distance to Fornax was derived using stars within  $\pm 2\sigma$  from the fiducial sequence. As shown in Sect. 4.4, this implies selecting the dominant stellar population in Fornax. Luminosity distributions were obtained both in  $V$  and in  $I$  by counting stars in 0.2 mag bins down to below the red clump. Since at these bright magnitudes our photometry is virtually complete, there was no need to correct the observed LF’s for incompleteness. Foreground and background contamination is not a concern, either, because the number of field objects in the proximity of the RGB is negligible.

The cutoff in the  $I$  luminosity function corresponding to the maximum luminosity reached by red giants before they ignite the He burning, has proven to be a good distance indicator (Madore & Freedman 1995; see also Salaris & Cassisi 1998). We measured the  $I$  magnitude of the RGB tip separately for our 4 Fornax fields, following the methods of Lee et al. (1993).

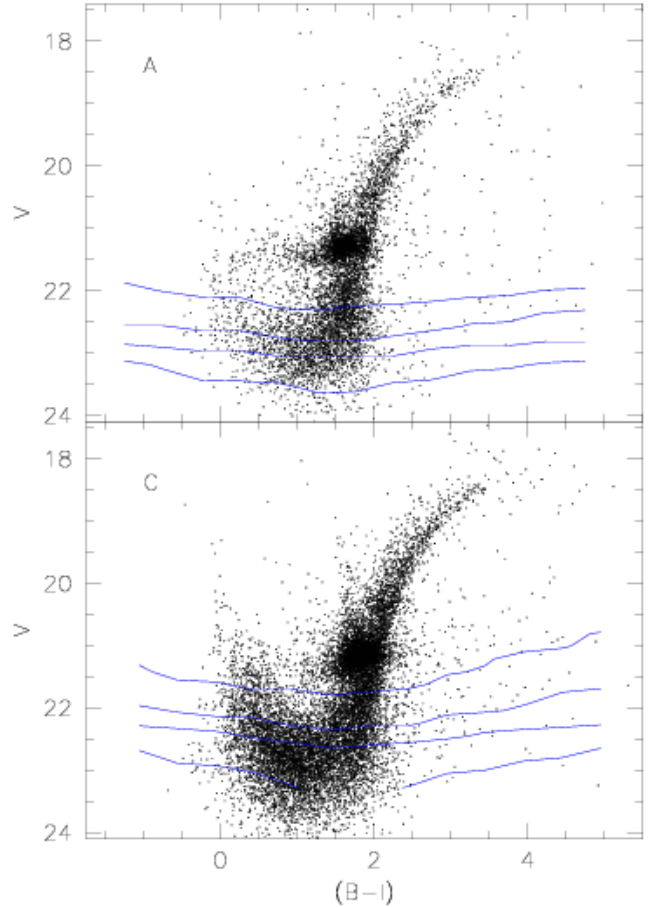


**Fig. 4.** A comparison of the color-magnitude diagrams in an outer and inner region of Fornax. Field A (top panel) is located about  $14'$  from the center of Fornax, while field C (bottom) samples an area near the galaxy center. The contour lines represent the 30%, 50%, 70% and 90% completeness levels of our photometry. Note that the completeness in the crowded field C is lower than in field A. The number of young main sequence stars and their helium-burning counterparts decreases from the inner to the outer field, allowing perceiving the bluer HB stars belonging to the oldest Fornax field population

The mean of the four values is  $\langle I_{\text{TRGB}} \rangle = 16.72 \pm 0.10$ . Although the scatter of the individual measurements is small ( $\sim 0.02$  mag), we have adopted a larger uncertainty to take into account both the intrinsic precision of the tip detection method, which is about a half of the 0.2 mag bin, and the zero point uncertainties.

We then calculated the distance to Fornax using the relations of Da Costa & Armandroff (1990). This procedure, often applied to derive the distance of dwarf galaxies, implicitly assumes that the  $I$  magnitude of the tip is little affected by age. Theoretical models indeed show a dependence of the tip luminosity on the age, but this is more pronounced for very metal-

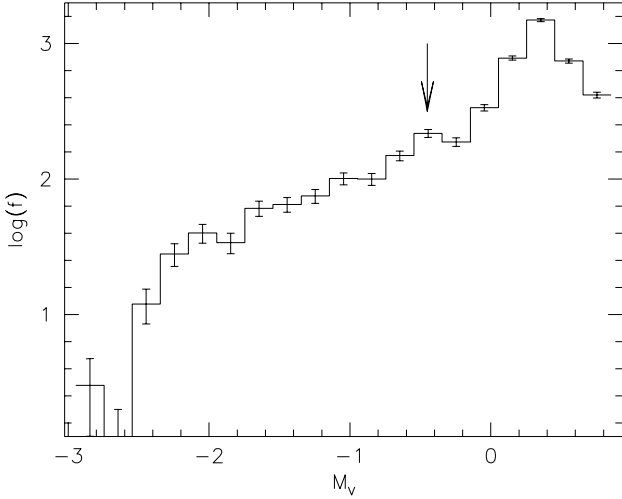


**Fig. 5.** The  $V$  RGB luminosity function of Fornax, showing the sharp cutoff at the RGB tip, the prominent red clump at  $M_V \approx +0.4$ , and the “AGB bump”, a clumping of intermediate age stars at the beginning of their AGB double-shell burning phase ( $M_V \approx -0.4$ )

poor populations ( $[\text{Fe}/\text{H}] < -1.7$ ) and ages younger than 5 Gyr (e.g., Caputo et al. 1999).

The relations of Da Costa & Armandroff (1990) give the  $I$  bolometric correction as a function of color of the stars near the RGB tip, and the bolometric luminosity of the tip as a function of metallicity. The dereddened color of the RGB tip in Fornax, calculated as the median  $(V - I)$  within 0.1 mag from the tip, is  $(V - I)_{0,\text{TRGB}} = 1.59 \pm 0.06$ , where the error reflects the scatter of the values obtained in our four fields plus the absolute zero point uncertainty. We adopted a reddening  $E_{B-V} = 0.03 \pm 0.03$  from Burstein & Heiles (1982), yielding  $E_{V-I} = 0.038 \pm 0.038$  and  $A_I = 0.058 \pm 0.058$ . The bolometric correction is then  $BC_I = 0.495 \pm 0.015$ , while a metallicity  $[\text{Fe}/\text{H}] = -1.39 \pm 0.15$  (cf. Sect. 4.3) implies  $M_{\text{bol}}^{\text{TRGB}} = -3.55 \pm 0.01$ . We thus obtain  $M_I^{\text{TRGB}} = -4.04 \pm 0.02$ , and a distance modulus  $(m - M)_0 = 20.70 \pm 0.12$ , corresponding to  $138 \pm 8$  kpc.

Previous distance estimates range from  $(m - M)_0 = 20.59 \pm 0.22$  (Buonanno et al. 1985) to 20.76 (Demers et al. 1990; Buonanno et al. 1999). Sagar et al. (1990) found  $(m - M)_0 = 20.7$ . The present estimate therefore confirms earlier results. This value is also consistent with the distance moduli of Fornax globular clusters (Buonanno et al. 1998), yielding an average modulus  $(m - M)_0 = 20.62 \pm 0.08$ .

Using this distance estimate, we plot in Fig. 5 the  $V$  luminosity function of the red giant stars in the inner region of Fornax. Besides the obvious red clump at  $M_V \simeq 0.4$ , we notice the small yet significant peak near  $V = 20.4$  that we identify with the AGB bump, a clustering of stars that occurs at the beginning of helium shell-burning evolution. Gallart (1998) has recently discussed the presence of this feature in the LMC and M31 where its location agrees with the prediction of stellar evolution

models (Bertelli et al. 1994). We have measured the location of the AGB bump in Fornax by performing a Gaussian fit to the LF in the region of the bump. We found  $V = 20.40 \pm 0.04$ , where the error is mainly set by the zero point uncertainty. This corresponds to a luminosity  $M_V \simeq -0.39 \pm 0.04$ , with an additional 0.1 mag uncertainty on the  $A_V$  extinction. Similarly, we measured a mean  $V$  magnitude for the red clump  $V_{\text{RC}} = 21.18 \pm 0.04$  mag, corresponding to  $M_V = +0.39$ . Thus the detected clump is  $0.78 \pm 0.06$  mag brighter in  $V$  than the red HB clump. For an assumed age of 5 Gyr and the mean metallicity of Fornax, these measurements confirm the identification with the AGB bump and rule out alternative identifications with the RGB bump. The RGB bump is expected to be near the HB level for a metallicity  $[\text{Fe}/\text{H}] \approx -1$  and age 5 Gyr (Alves & Sarajedini 1999). In Lynds 113, a 5 Gyr old cluster in the Small Magellanic Cloud having metallicity comparable with that of Fornax, the RGB bump is found to be  $\sim 0.15$  mag brighter than HB stars in the same cluster (Mighell et al. 1998). Clearly, stars in the RGB bump will be outnumbered by the overwhelming red clump. Observational data like those presented here for the Fornax dwarf are important to constrain evolutionary models, which in turn are necessary to interpret the stellar population of Local Group galaxies.

#### 4.2. Distance based on the old horizontal branch

An independent estimate of the distance to Fornax was obtained from the mean level of its old-HB field stars. The mean magnitude of the HB was measured by fitting a Gaussian to the  $V$  mag distribution of the stars in the range  $21.2 < V < 21.7$ ,  $1.1 < B - I < 1.5$ . We necessarily included only the red part of the  $\text{HB}_{\text{OLD}}$ , since the bluer horizontal-branch stars appear to be mixed with the blue stars on the young main sequence. Note, however, that we do not include any RC stars (which are brighter than the  $\text{HB}_{\text{OLD}}$  and RR Lyrae variables). The mean level of the red HB is  $V_{\text{HB}} = 21.37 \pm 0.04$ , where the uncertainty reflects the scatter of the values measured in the different fields (larger than the formal error on the mean magnitude), and the systematic error of the  $V$  zero point. Buonanno et al. (1998) found a mean level  $V_{\text{HB}} = 21.25 \pm 0.05$  for the  $\text{HB}_{\text{OLD}}$  of four globular clusters in Fornax.

Using this value for  $V_{\text{HB}}$ , and  $A_V = 3.2 E(B - V) = 0.096$ , we calculated the distance modulus of Fornax on the Lee et al. (1990) distance scale, using their relation for the absolute visual magnitude of RR Lyrae variables,

$$M_V^{\text{RR}} = 0.17 [\text{Fe}/\text{H}] + 0.82 \quad (6)$$

for a helium abundance of  $Y = 0.23$ .

Assuming for red HB stars the relatively metal-rich nominal metal content of RGB stars,  $[\text{Fe}/\text{H}] \approx -1.4$ , this relation would give  $M_V^{\text{RR}} = 0.59$  mag and a distance modulus  $(m - M)_0 = 20.69 \pm 0.04$  for a population with age comparable to that of Galactic globular clusters. This uncertainty includes internal and photometric errors only. However, the mean metallicity of the old-HB stars is probably lower. If the old population in Fornax is relatively metal-poor, of the order



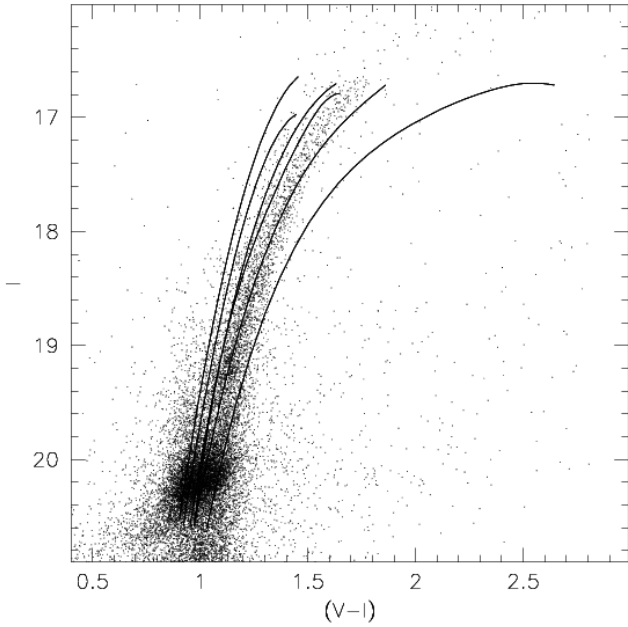


**Fig. 6.** A comparison of our total color-magnitude diagram of Fornax with the giant branches of template Galactic globular clusters from Da Costa & Armandroff (1990), scaled to the distance and reddening of Fornax. The globular clusters span a metallicity range from  $[\text{Fe}/\text{H}] = -2.2$  to  $[\text{Fe}/\text{H}] = -0.7$

$[\text{Fe}/\text{H}] \approx -1.8$  (as we suggest in Sect. 4.5), the relation given by Lee et al. (1990) would imply  $M_V^{\text{RR}} = 0.51$  mag and a distance modulus  $(m - M)_0 = 20.76 \pm 0.04$ . The level of the red HB (distinct from the clump) is probably the result of contributions from stars in a range of ages and metallicities. For this reason we refrained from applying any uncertain correction to convert the measured mean magnitude of the red  $\text{HB}_{\text{OLD}}$  to an equivalent magnitude of RR Lyrae variables. Further, this distance modulus based on the HB level is affected by the uncertainties on the luminosity of HB stars as a function of age and metallicity. A discussion of the alternative distance scales, however, is beyond the scope of this paper.

This measurement of the distance to Fornax based on its old horizontal branch star luminosity confirms the distance modulus estimated from the RGB tip. This consistency is not unexpected, since both the RGB tip method of DA90 and the HB absolute magnitude obtained for the  $\text{HB}_{\text{OLD}}$  are based on the distance scale of Lee et al. (1990). These two distance measurements use  $I$  and  $V$  magnitudes, respectively, which are observationally independent.

#### 4.3. Mean abundance and age

The mean metal abundance of the bulk of the Fornax population was derived by direct comparison of the red giant branch in the  $I$ ,  $(V - I)$  color-magnitude diagram with the ridge lines of globular clusters from Da Costa & Armandroff (1990) (see Fig. 6). Our procedure is fully described in Paper I and II, and

is only briefly outlined here. In short, we calculated the average color shift,  $\delta(V - I)_0$ , between the Fornax RGB and the Galactic cluster fiducial loci. An interpolation of the relation between the mean color shifts and the globular cluster metallicities (actually a quadratic fit) provides an estimate of  $[\text{Fe}/\text{H}]$  for the dwarf spheroidal. This procedure was applied to the  $2\sigma$ -selected RGB sample (cf. Sect. 4.1), in two luminosity intervals ( $-4.0 < M_I < -3.0$  and  $-3.0 < M_I < -2.0$ ), yielding a metallicity  $[\text{Fe}/\text{H}] = -1.45 \pm 0.11$  and  $[\text{Fe}/\text{H}] = -1.33 \pm 0.15$  dex, respectively. The mean of the abundances determined in these two magnitude bins was adopted as our final estimate. The resultant value,  $[\text{Fe}/\text{H}] = -1.39 \pm 0.15$ , is in good agreement with previous work. We find no evidence for a metallicity gradient among the regions studied here, to within the errors.

However, the measurements of mean abundance based on the color of the RGB are subject to the well-known difficulty in disentangling the effects of age and metallicity on the effective temperature of red giant stars (the “age-metallicity degeneracy”). Thus we need to estimate the mean age of Fornax before discussing further its mean metal abundance. When compared with the predictions of stellar evolution models (e.g., Bertelli et al. 1994; Caputo et al. 1995), the position of core He burning stars in color-magnitude diagrams may provide a useful age indicator (e.g., Caputo et al. 1999; Girardi 1999; and references therein). The RC comprises core helium-burning stars of different ages, so that its location bears information on the *mean age* of the intermediate age population, weighted by the age distribution function. Thus, similarly to what we had done for the HB, we measured the mean  $(B - I)$  color in addition to the  $V$  luminosity for the red clump. The mean magnitude, already reported above, is  $V_{\text{RC}} = 21.18 \pm 0.04$  mag, corresponding to  $M_V = +0.39$ , in excellent agreement with Demers et al. (1994). This means that the RC is  $0.19 \pm 0.06$  mag more luminous in  $V$  than the old HB stars, a value that appears consistent with the difference in age of a 13 Gyr old population and a 5 Gyr old bulk component (see Caputo et al. 1999). The clump is quite extended in luminosity ( $\sim 0.6$  mag), comparable with that of Carina (Hurley-Keller et al. 1998), but less than that of Leo I (cf. Gallart et al. 1999a). The mean color is  $\langle B - I \rangle_{\text{RC}} = 1.79 \pm 0.04$ . The uncertainties include the field-to-field scatter, comparable with the photometric measurement errors, and the zero-point uncertainty. The relation  $(V - I) = 0.457(B - I) + 0.147$ , obtained from a linear fit to the color-color relations for the Fornax red giants in the range  $1.0 < (B - I) < 3.5$ , yields  $\langle V - I \rangle_{\text{RC}} = 0.965$ . This value shows excellent agreement with the results of Buonanno et al. (1999). By fitting a parabola to the fiducial points of the RGB, we estimated the interpolated RGB color at the RC level ( $V - I \simeq 1.07$  mag), a value also confirmed by inspection of the WFPC2 color-magnitude diagram (Buonanno et al. 1999). The difference in color between the red clump and red giant stars at the same luminosity is then  $\delta_{(V-I),\text{RC}} = 0.10$  mag, with an estimated uncertainty of  $0.02$  mag. This result can be compared with the model predictions of Girardi (1999; and priv. comm.) based on the models of Girardi et al. (1999), which are in accord with the empirical calibration of Hatzidimitriou

**Table 3.** Observed and instrumental color dispersions  $\sigma_{(B-I)}$  for the main component of the RGB color distributions in fields A and C.

$I$	$\sigma_A$	$\sigma_C$	$\sigma_A(\text{instr})$	$\sigma_C(\text{instr})$	$\sigma_{0,A}$	$\sigma_{0,C}$
17.20	0.082	0.067	0.024	0.029	0.078	0.060
18.20	0.063	0.077	0.036	0.042	0.052	0.065
19.20	0.088	0.093	0.061	0.073	0.063	0.058

(1991). For a metallicity  $Z=0.001$  (but  $\delta_{(V-I),\text{RC}}$  is relatively independent of abundance for metal-poor populations) our result is consistent with a mean age of the order  $5.4 \pm 1.7$  Gyr. This value is close to the estimate of Sagar et al. (1990), based on best fitting of Yale isochrones, and definitely larger than the age estimated by Demers et al (1994). Most interestingly, the mean age obtained from the clump location appears to be consistent with the presence of MS evolved stars in the same age interval, as observed with HST (Buonanno et al. 1999). This results is quite encouraging for application of this age indicator to more distant Local Group galaxies, whose main-sequence turnoff cannot be directly measured.

If we now assume a mean age of approximately 5 Gyr for the bulk of the Fornax stars, the observed RGB color would imply a metallicity significantly larger than the formal result obtained above from a comparison with globular clusters. We have estimated the effects of age by comparing theoretical isochrones of different ages (e.g., 5 and 15 Gyr) at a given metallicity (from Bertelli et al. 1994). By measuring the  $(V-I)$  colors at  $M_I = -2.5$  predicted by model isochrones with  $Z=0.001$  ( $[\text{Fe}/\text{H}] = -1.3$ ), we find that a 5 Gyr isochrone is bluer by  $\sim 0.09$  mag than a 15 Gyr model isochrone. This effect mimics a metallicity difference of  $\sim 0.4$  dex using the fiducial loci of globular clusters (cf. Paper II; Caputo et al. 1999; Gallart et al. 1999a). Thus, if the body of Fornax stars is  $\sim 5$  Gyr old, the measured location of the peak of the RGB is necessarily indicative of a higher mean metallicity, of the order  $[\text{Fe}/\text{H}] = -1.0$  (clearly the correction is somewhat model dependent). We regard this value as the most appropriate estimate of the mean metal abundance of the dominant stellar population in Fornax. With this correction, the Fornax metallicity turns out to be very close to that of Sagittarius, a dSph which has a comparable total luminosity (e.g., Bellazzini et al. 1999).

#### 4.4. The color distribution of Fornax red giants

One of the main results of this paper, made possible by the size of our stellar sample and photometric baseline, is a detailed analysis of the color distribution function (CDF) of the red giant stars in Fornax. Fig. 7 shows the distribution of the  $(B-I)$  color residuals about a preliminary fiducial sequence, in the magnitude range  $17.7 \leq I \leq 18.7$  ( $-3 < M_I < -2$ ), for the inner and outer field. While these histograms confirm

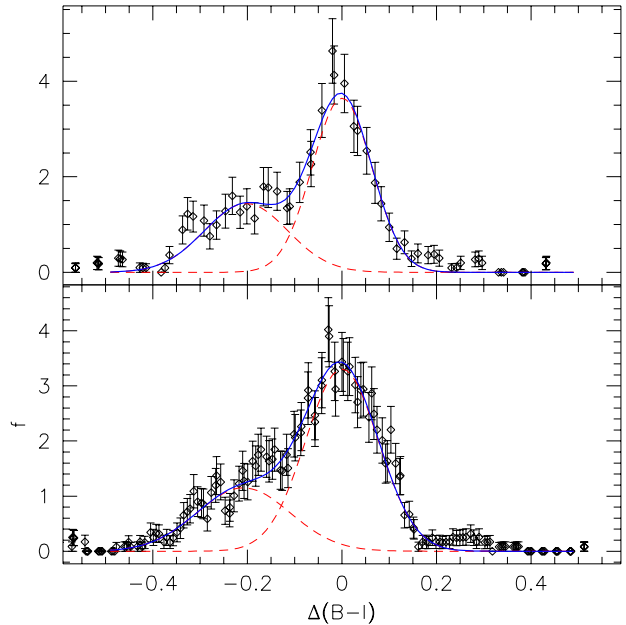


**Fig. 7.** The color distribution of the red giant stars in Fornax, plotted separately for the inner (bottom panel) and outer region (top panel). The histograms represent the distributions of the color residuals of individual stars from a median RGB fiducial sequence, in the magnitude interval  $17.7 \leq I \leq 18.7$ . Error bars represent Poisson errors. The color distribution is quite well fitted by the sum (continuous line) of two Gaussian functions (dashed lines) suggesting a two-component model for the metallicity (or age) distribution of Fornax stars.

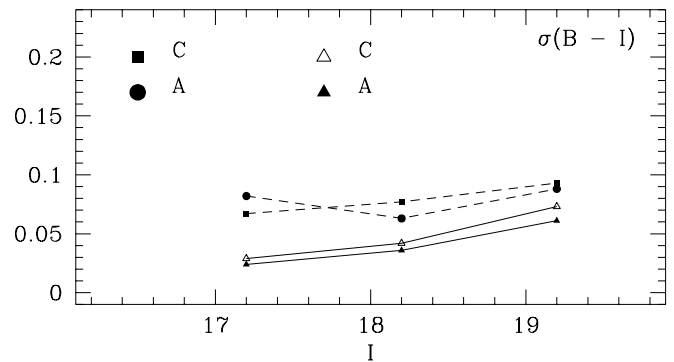


**Fig. 8.** Plot of the measured color scatter  $\sigma_{(B-I)}$  of the *principal* RGB component in our fields A and C (circles), compared with instrumental dispersions (triangles).

the well-known wide color range of the RGB stars in Fornax (e.g., Buonanno et al. 1985; Sagar et al. 1990; Grebel et al. 1994; Beauchamp et al. 1995), they also show that the color distributions cannot merely be described using a single “color dispersion”. Rather, the CDF is more appropriately described as roughly bimodal, showing a principal peak and a bluer com-

ponent extending to  $\Delta(B - I) \simeq -0.4$ . This color distribution function is quite well modeled by the sum of two Gaussians. The main component of the distribution represents the bulk of the red giant population, a mix of old and (mostly) intermediate-age stars. The secondary peak is centered at about  $\Delta_{B-I} = -0.20$ .

On the other hand, we notice a relatively well-defined cut-off on the red side of the RGB, indicating the lack of any significant metal-rich component similar to the stellar population of 47 Tuc, or even less metal-rich if we assume a mean age younger than that of Milky Way globular clusters. This absence sets an important constraint for modeling the chemical enrichment of the Fornax dwarf. Both components are wider than accounted for by instrumental errors. The dispersions of the two components, in the luminosity range  $-3 < M_I < -2$ , are  $\sigma_{B-I}^a = 0.063$  (central peak) and  $\sigma_{B-I}^b = 0.088$  (blue component) in the inner region, and  $\sigma_{B-I}^a = 0.077$ ,  $\sigma_{B-I}^b = 0.099$  in the outer field. Table 3 gives the observed dispersions for the main component of the Fornax field population for the inner and outer region in 3 magnitude intervals. Also given in Table 3 are the instrumental errors  $\sigma(B - I)$  obtained by fitting a Gaussian to the color residuals of artificial stars, exactly in the same way as for the real data. The observed and instrumental dispersions are also compared in Fig. 8. The intrinsic  $(B - I)$  color dispersions, calculated as the quadratic difference between the observed and the instrumental scatter, are given in the last two columns of Table 3. In the luminosity interval  $-3 < M_I < -2$  the intrinsic color spread of the main RGB population is  $\sigma_0(B - I) = 0.06 \pm 0.01$  mag. Using again the color-color relations for the Fornax red giants to convert  $(B - I)$  color spreads into equivalent dispersions in  $(V - I)$ , and the calibration of RGB color shifts as a function of metal abundance variations, we obtained a metallicity spread  $\sigma_{[\text{Fe}/\text{H}]} = 0.12 \pm 0.02$  dex for the dominant field population.

Then the ( $2\sigma$ ) metallicity range for the bulk population of Fornax would be approximately  $-1.65 < [\text{Fe}/\text{H}] < -1.15$ , or  $-1.25 < [\text{Fe}/\text{H}] < -0.75$  if a correction for the mean age is applied. This intrinsic metallicity range is significantly lower than the abundance spread quoted by most previous studies for the red giant branch as a whole. According to Beauchamp et al. (1995), the total range in  $[\text{Fe}/\text{H}]$  is 0.8 dex, comparable to that found by Sagar et al. (1990) and Grebel et al. (1994). A smaller spread ( $\lesssim 0.1$  dex) was found by Geisler (1994). This discrepancy probably results from the coarser metallicity resolution of the colors employed in past studies, with the notable exception of the Washington colors of Geisler (1994). We conclude that a small abundance spread seems in fact more appropriate to describe the intermediate-age field population in Fornax. While the metallicity dispersion given above is comparable to that of Leo I (e.g., Gallart et al. 1999a), it appears to be smaller than the abundance spread found in the majority of dwarf spheroidal galaxies (Da Costa 1998; Mateo 1998). In a few cases, wide range in metallicity has been confirmed by low- and high-dispersion spectroscopy (e.g., Coté et al. 1999; Shetrone et al. 1998). The mean value of the metallicity spread for Galactic dSph and satellites of M 31 is  $0.37 \pm 0.03$  dex (Coté

et al. 1999). Had we considered our Fornax RGB color distribution as a whole, we would have obtained a metallicity spread of the same order ( $-2.0 < [\text{Fe}/\text{H}] < -0.7$ ,  $\pm 2\sigma$  range), in good agreement with previous studies.

Since age is known to affect the RGB color,  $[\text{Fe}/\text{H}]$  dispersions derived by the width of the giant branch should be taken with caution in view of a possible contribution of an age spread. As argued above, an age range of the order 5 Gyr (which is that of stars making up the main RGB) is sufficient to mimic a metallicity range of  $\pm 0.1$  dex. Thus we might assume that the width of the RGB main component is entirely due to the age spread of its populations. The situation is more complex, though, and the effects of a metallicity and age range on the color distribution depend on the details of the star formation and chemical enrichment history. Successive stellar generations are expected to be progressively more metal-enriched, so that younger stars (implying a bluer RGB) will generally have higher metal abundance (leading to a redder RGB). The two effects – of a younger age and higher metallicity – will act in opposite directions, and may even compensate each other as it appears to be the case for Carina (Smecker-Hane et al. 1994). Similarly to Carina, the abundance spread we have found for the dominant population of Fornax may represent a *lower limit* (see also Paper II; Gallart et al. 1999a; for similar considerations for other dSph's). This issue shall be more quantitatively investigated in a following paper.

We return now to discuss the nature of the population making up the blue tail of the CDF, which is until now far from established. Qualitative examination of the CMD's is not sufficient to establish whether the blue tail of the CDF represents an old, metal-poor population, or is made up of young red AGB stars. However, we will show in Sect. 4.5 that there is definite evidence that the bluer RGB stars are old and metal-poor, which implies that the extended color distribution shown in Fig. 7 can be interpreted as a metallicity distribution. In conclusion, a model involving two populations seems to provide a good description of the star content of the Fornax dSph, with the older population having  $[\text{Fe}/\text{H}] = -1.82$  with a dispersion of 0.20 dex, and the dominant, intermediate-age population with  $[\text{Fe}/\text{H}] \approx -1.0 \pm 0.15$ . Our large-field data confidently rule out the presence of a distinct metal-rich population with abundance comparable to that of 47 Tuc, even accounting for a mean age of 5 Gyr for the Fornax bulk population.

This complexity is common to most of the other dwarf spheroidals. For example, two distinct star formation epochs have been recently revealed in Sculptor by Majewski et al. (1999). In this galaxy, a detailed analysis of the RGB morphology showed the presence of two distinct RGB bumps consistent with the presence of a metal-poor population of  $[\text{Fe}/\text{H}] \sim -2.3$ , and a population of  $[\text{Fe}/\text{H}] \sim -1.5$ . Also the recent study of the star formation history of Leo I by Gallart et al. (1999b) indicate that most of the star formation activity (80%) occurred between 7 and 1 Gyr (mean 4 Gyr) while the contribution of the older phase was small. A wide metallicity range and a composite population, although with a higher mean abundance, has also been inferred in the Sagittarius dSph, a galaxy similar in many

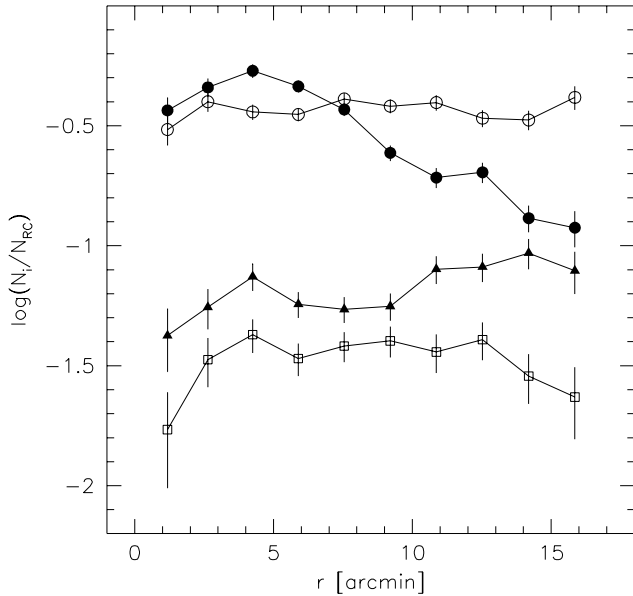


**Fig. 9.** Radial trends in the fraction of young main sequence stars (filled circles), HB stars (triangles), stars on the blue-RGB (squares) and RGB (open circles) relative to the number of red clump stars. The logarithm of the ratios is plotted against the effective distance from the Fornax center.

**Table 4.** Star counts normalized to 100 stars in the red clump

$r'$	HB	BL	yMS	bRGB	RGB
1.2	4.2	7.0	36.6	1.7	30.5
2.6	5.5	6.3	45.7	3.3	39.8
4.2	7.4	9.3	53.6	4.3	36.1
5.9	5.7	7.4	46.2	3.4	35.2
7.5	5.4	5.9	37.0	3.8	40.9
9.2	5.6	5.2	24.4	4.0	38.1
10.9	8.0	6.0	19.2	3.6	39.5
12.5	8.2	6.1	20.2	4.1	34.0
14.2	9.3	4.4	13.0	2.9	33.4
15.9	7.9	5.7	11.9	2.3	41.5

respects to Fornax (Bellazzini et al. 1999). Also, the metallicity distribution of stars in the small elliptical M 32 shows a metal-rich peak ( $[\text{Fe}/\text{H}] \simeq -0.2$ ) with a low-metallicity tail extending to about  $[\text{Fe}/\text{H}] \sim -1.5$  (Grillmair et al. 1996). It is also interesting to note the analogy with the extremely broad metallicity range found in the halo of the nearby elliptical NGC 5128 (Harris et al. 1998), where the shape of the metallicity distribution suggested a two-phase *in situ* model.

#### 4.5. Population gradients

A comparison of the color-magnitude diagram in the different regions in this study provided important clues regarding the origin of the stellar populations in Fornax, and in particular on the nature of its complex red giant branch. Were the bluer RGB stars old and metal-poor, one would expect a higher fraction of them in the outer fields, on the basis of the population gradient detected by SHS98. Clearly the opposite finding, i.e. a larger RGB blue tail in the inner regions, would indicate a connection to the more recent bursts of star formation.

In order to measure the radial gradient in the stellar populations in Fornax, stars in different evolutionary phases were counted separately in different radial bins. The CMD regions chosen for counts include the red clump, the red part of the  $\text{HB}_{\text{OLD}}$ , the blue-loop helium-burning stars (BL), the young main sequence (yMS), and the red giants (those in the mainstream giant branch, RGB, and in the bluer component, bRGB).

The reader is referred to the boxes outlined in Fig. 2. The results of star counts are presented in Table 4, where we list the effective galactocentric distance and the percentage of stars in all the CMD regions relative to the number of RC stars.

The fraction of young main sequence, old HB, blue-RGB and mainstream RGB stars are also plotted on a logarithmic scale in Fig. 9. As previously noticed by SHS98, the young stars are more centrally concentrated than the dominant intermediate age component, indicating that recent star formation took place preferentially in the central regions. The counts on the RGB as expected follow those of RC stars. Conversely, the HB stars are preferentially found in the outer regions.

Most importantly, the bluer RGB stars *closely follow the radial trend of the horizontal-branch stars* (Fig. 9). This result unambiguously demonstrates that the sparse sequence on the blue side of the Fornax RGB belongs to the *old and metal-poor* population ( $\gtrsim 10$  Gyr) along with the old-HB stars and RR Lyrae variables.

## 5. Summary and conclusions

We have presented a large area study of the field population in the Fornax dwarf spheroidal galaxy, based on *BVI* data for about 40000 stars. The size of our sample, together with the wide photometric baseline employed in this work, provide new information on the stellar content of Fornax.

One of the most distinctive features in our diagrams is the conspicuous young main sequence. In this paper we have shown that the plume of stars just above the red clump is made up of intermediate mass stars ( $2.4\text{--}2.9 M_{\odot}$ ) burning helium in the core, counterparts of the young main sequence stars in the age range 0.3–0.4 Gyr. The comparison with isochrones suggests us that these blue-loop stars must be as metal-rich as  $[\text{Fe}/\text{H}] \sim -0.7$ , which represents an important constraint for the metal enrichment history in Fornax.

An extended upper AGB tail and a prominent red HB clump testify the presence of a dominant intermediate-age population in the age range 2–10 Gyr, corresponding to  $0.9\text{--}1.4 M_{\odot}$  stars.

From the difference in the mean ( $V - I$ ) colors of the red clump and the RGB at the same luminosity, we have estimated a mean age  $5.4 \pm 1.7$  for the bulk of the intermediate-age population in Fornax, in agreement with the morphology of the MS turnoffs in WFPC2 color-magnitude diagrams (Buonanno et al. 1999). This suggests that the location of the red HB clump may indeed prove to be a useful age indicator for distant LG galaxies.

About 0.2 mag below the red clump, an extended HB is indicative of an old population. In particular, our data point to the presence of blue HB stars in the outer regions. Together with previous detection of RR Lyrae, this provides evidence for a minority field population that is as old and metal-poor as that in the Fornax globular clusters. The Fornax dSph clearly started forming stars in a halo nearly at the same epoch when most of its surrounding clusters were formed.

Evolutionary phases that gave barely discernible features in small field observations are easily measurable in our color-magnitude diagrams. We could reliably measure the AGB bump, a small clump produced by a clustering of stars at the base of the AGB, at  $M_V \simeq -0.4$ . Measurements of such minor evolutionary features may provide useful tests of stellar models for stars of different masses and metallicities.

The sharp cutoff in the luminosity function of Fornax has been used to estimate its distance using the RGB tip method. The corrected distance modulus of Fornax,  $(m - M)_0 = 20.70 \pm 0.12$ , agrees with previous determinations. This estimate is confirmed by the mean level of old horizontal-branch stars. By measuring the average magnitude of the red HB (distinct from the red clump) we estimated a distance modulus  $(m - M)_0 = 20.76 \pm 0.12$  on the distance scale of Lee et al. (1990).

Fornax, as many other dSph, has been known for a long time to have a wide RGB color distribution. The “color scatter” has been usually taken to represent an abundance spread. We have analyzed in detail the color distribution of the red giant stars across the fiducial line, and found that it is reasonably well fitted by a two-component model. This approximately bimodal distribution is remarkably similar in all fields. About 70% of the red giants belong to an intermediate-age RGB component which is itself wider than expected from instrumental errors. By comparing the bulk of the Fornax RGB with the ridge lines of standard globular clusters, we have estimated a mean metallicity  $[\text{Fe}/\text{H}] = -1.39 \pm 0.15$ . This nominal value should be corrected for the age difference between the Fornax population and the Milky Way globulars. Accounting for an age difference of 10 Gyr, we find an *age-corrected* mean metallicity  $[\text{Fe}/\text{H}] = -1.0 \pm 0.15$  for the dominant intermediate-age population of Fornax. Interestingly, this is also the metallicity found for Sagittarius, the nearest Milky Way dSph satellite that has luminosity comparable to that of Fornax. The *intrinsic* color scatter of stars in the RGB main component is  $\sigma_{(B-I)} = 0.06 \pm 0.01$  mag implying a relatively modest metallicity spread  $\sigma_{[\text{Fe}/\text{H}]} = 0.12 \pm 0.02$  dex. Then the  $(2\sigma)$  metallicity range for the bulk population of Fornax is  $-1.25 < [\text{Fe}/\text{H}] < -0.75$  if a correction for the mean age is applied. The secondary compo-

nent or “bluer tail” is also quite broad. In principle, these bluer stars could be either young or old and metal-poor.

Star counts of different subpopulations at various locations confirm and extend the evidence for radial population gradients emerged in previous studies. Recent star formation is clearly concentrated in the central regions, though with some degree of asymmetry (e.g., SHS98). Old stars are more easily seen in the outer fields. A blue HB population can be noticed in our outermost field, coming from the minority old, metal-poor field component. The stars populating the blue side of the wide RGB closely follow the spatial distribution of the old-HB stars. This is perhaps our most important finding, since it demonstrates that the bluer RGB stars are themselves old and metal-poor, and clearly establishes the nature of the wide RGB of Fornax. Thus the roughly bimodal color distribution can be interpreted as a metallicity distribution, implying that the bulk of the Fornax galaxy was built during two rather distinct star-forming epochs. The older population has  $[\text{Fe}/\text{H}] \approx -1.8$  dex with  $(\pm 2\sigma)$  and an wide abundance range  $-2.2 < [\text{Fe}/\text{H}] < -1.4$ .

The emerging picture is one in which the evolution of Fornax is characterized by two major star formation epochs, each consisting of many episodes. The first episode took place at an early epoch, being presumably coeval to the birth of the old galactic globular clusters, from metal-poor gas. After a relatively quiescent period, Fornax formed the bulk of stellar populations between 7 and 2.5 Gyr ago from the pre-enriched gas. Star formation continued at a lower rate in the central regions until as recently as  $10^8$  yr ago. The modest internal abundance spread found in each main population seen in the metallicity distribution, and the different metallicities of populations of different age, trace the progressive metal enrichment and represent the basis for an age-metallicity relation in Fornax. The constraints found in this paper provide the physical input for a quantitative analysis of the star formation and chemical enrichment history of Fornax, which will be done in a forthcoming study using the methods of stellar population synthesis.

*Acknowledgements.* We thank L. Girardi for useful discussions and for kindly providing us with unpublished theoretical red clump colors. Dr. P.B. Stetson is thanked for helpful comments on the manuscript. I. S. acknowledges support from ANTARES, an astrophysics network funded by the HCM program of the European Community.

## References

- Aaronson M., Mould J.R., 1980, ApJ 240, 804
- Aaronson M., Mould J.R., 1985, ApJ 290, 191
- Alves D.R., Sarajedini A., 1999, ApJ 511, 225
- Aparicio A., Gallart C., Chiosi C., Bertelli G., 1996, ApJ 469, L97
- Aparicio A., Dalcanton J.J., Gallart C., Martínez-Delgado D., 1997, AJ 114, 1447
- Azzopardi M., Breysacher J., Muratorio G., Westerlund, B.E. 1999, in IAU Symp 192, The Stellar Content of Local Group Galaxies, eds. P. Whitelock R. Cannon (ASP, San Francisco), in press
- Beauchamp D., Hardy E., Suntzeff N.B., Zinn R., 1995, AJ 109, 1628
- Bellazzini M., Ferraro F.R., Buonanno R., 1999, MNRAS 307, 619
- Bersier D., Wood P.R., 1999, IAU Symp. 192, The Stellar Content of Local Group Galaxies, P. Whitelock R. Cannon Eds. (ASP, San Francisco), in press

- Bertelli G., Bressan A., Chiosi C., Fagotto F., Nasi E., 1994, *A&AS* 106, 275
- Buonanno R., Corsi C. E., Fusi Pecci F., Hardy E., Zinn R., 1985, *A&A* 152, 65
- Buonanno R., Corsi C.E., Zinn R., et al., 1998, *ApJ* 501, L33
- Buonanno R., Corsi C.E., Castellani M., et al., 1999, *AJ* 118, 1671
- Burstein D., Heiles C., 1982, *AJ* 87, 1165
- Caputo F., Castellani V., Degl'Innocenti S., 1995, *A&A* 304, 365
- Caputo F., Cassisi S., Castellani M., Marconi G., Santolamazza P., 1999, *AJ* 117, 2199
- Cole A.A., Tostoy E., Gallagher J.S., et al., 1999, *AJ* 118, 1657
- Coté P., Oke J.B., Cohen J.G., 1999, *AJ* 118, 1645
- Da Costa G.S., 1998. In Aparicio A., Herrero A., Sanchez F. (eds.), *Stellar Astrophysics for the Local Group*, Cambridge University Press, Cambridge, p. 351
- Da Costa G.S., Armandroff T.E., 1990, *AJ* 100, 162
- Danziger I.J., Webster B.L., Dopita M.A., Hawarden T.G., 1978, *ApJ* 220, 458
- Demers S., Grondin L., Kunkel W.E., 1990, *PASP*, 102, 632
- Demers S., Irwin M.J., Kunkel W.E. 1994, *AJ* 108, 1648
- Eskridge P.B., 1988, *AJ* 96, 1614
- Frogel J.A, Blanco V.M., McCarthy M.F., Cohen J.G., 1982, *ApJ* 252, 133
- Gallart C., 1998, *ApJ* 495, L43
- Gallart C., Freedman W. L., Mateo M., et al., 1999a, *ApJ* 514, 665
- Gallart C., Freedman, W. L., Aparicio A., Bertelli G., Chiosi C., 1999b, *AJ* in press
- Geisler D., 1994, In: Layden A., Smith R.C., Storm J. (eds) Proc. 3rd CTIO/ESO Workshop, The Local Group: Comparative and Global Properties. ESO, Garching, p. 141
- Girardi L., 1999, *MNRAS* 308, 818
- Girardi L., Bressan A., Bertelli G., Chiosi C., 1999, *A&AS*, in press
- Gizis J.E., Mould J.R., Djorgovski S., 1993, *PASP* 105, 871
- Gratton R.G., Ortolani S., Richter O.G., 1986, *Mem. SAI* 57, 561
- Grebel E.K., Roberts W.M., van de Rydt F., 1994, In: Layden A., Smith R.C., Storm J. (eds) Proc. 3rd CTIO/ESO Workshop, The Local Group: Comparative and Global Properties. ESO, Garching, p. 148
- Grillmair C.J., Lauer T.R., Worthey G., et al., 1996, *AJ* 112, 1975
- Harris G.L.H., Harris W.E., Poole G.B., 1998, *AJ* 117, 855
- Hatzidimitriou D., 1991, *MNRAS* 21, 545
- Held E.V., Saviane I., Momany Y., 1999, *A&A* 345, 747 (Paper II)
- Hodge P.W., 1961, *AJ* 66, 249
- Hurley-Keller D., Mateo M., Nemeč J., 1998, *AJ* 115, 1840
- Landolt A. U., 1992, *AJ* 104, 340
- Lee M. G., Freedman W. L., Madore B. F., 1993, *ApJ* 417, 553
- Lee Y.W., Demarque P., Zinn R., 1990, *ApJ* 350, 155
- Lundgren K., 1990, *A&A*, 233, 21
- Madore B. F., Freedman W. L., 1995, *AJ* 109, 1645
- Majewski S.R., Siegel M.H., Patterson R.J., Rood R.T., 1999, *ApJ* 520, L33
- Maran S.P., Gull T.R., Stecher T.P., Aller L.H., Keyes C.D., 1984, *ApJ* 280, 615
- Mateo M., 1998, *ARA&A* 36, 435
- Mighell K.J., Sarajedini A., French R.S., 1998, *AJ* 116, 2395
- Minniti D., Zijlstra A.A., Alonso M.V., 1999, *AJ* 117, 881
- Sagar R., Hawkins M.R.S., Cannon R.D., 1990, *MNRAS* 242, 167
- Salaris M., Cassisi S., 1998, *MNRAS* 298, 166
- Saviane I., Held E.V., Piotto G., 1996, *A&A* 315, 40 (Paper I)
- Shetrone M.D., Bolte M., Stetson P.B., 1998, *AJ* 115, 1888
- Smecker-Hane T. A., Stetson P. B., Hesser J. E., Lehnert M. D., 1994, *AJ* 108, 507
- Smith E.O., Rich R.M., Neill J.D., 1998, *AJ* 115, 2369
- Stetson P. B., 1987, *PASP* 99, 191
- Stetson P.B., Hesser J.E., Smecker-Hane T.A., 1998, *PASP* 110, 533 (SHS98)
- Westerlund B.E., Edvardsson B., Lundgren K., 1987, *A&A* 178, 41
- Young L.M., 1999, *AJ* 117, 1758